

# Computational study of natural convection in a nano-fluid filled enclosure containing pair of heater and cooler

Azzabakh Aniss, Feddaoui M'barek, Meftah Hicham

Laboratoire Génie Energie, Matériaux et Systèmes (LGEMS)  
Ecole Nationale des Sciences Appliquées ENSA, B.P. 1136, Agadir – Morocco

---

**Abstract:** The present paper deals to the numerical study of natural convection heat transfer of CuO-water nanofluid inside a square enclosure containing a heater and a cooler with isothermal walls of  $T_h$  and  $T_c$  ( $T_h > T_c$ ) respectively. A computer code, based on the finite volume method and the SIMPLER algorithm, is used to solve the Two-dimensional Navier–Stokes and energy. This code has been validated with comparison between the obtained results and those of Arefmanesh et al. [15].

To analyze the effects of pertinent parameters such the Rayleigh number, the solid volume fraction on the fluid flow and heat behaviors, the present work report the convection phenomenon by means of streamlines, isotherms, and velocity profiles, with a special attention to the Nusselt number.

The results show that the overall mean Nusselt number is an increasing function of the Rayleigh number and the nanoparticles volume fraction.

**Keywords:** Cooler, Enclosure, Finite volume, Heater, Nanofluid, Natural convection.

---

## 1. Introduction

Convective heat transfer in nanofluids, which are a suspension of nano-sized solid particles in a base fluid, occurs in many engineering applications such as the cooling systems of electronic components, building and thermal insulation systems, the built-in-storage solar collectors, the nuclear reactor systems, the food storage industry and the power plant [1].

Free convection heat transfer inside nanofluid filled rectangular cavities with different boundary conditions on the side walls have been studied by many researchers. A numerical study of natural convection of copper–water nanofluid in a two-dimensional enclosure was conducted by Khanafer et al. [2]. It was found in any given Grashof number, heat transfer in the enclosure increased with the volumetric fraction of the copper nanoparticles in water. Similar results were found in work of Jou and Tzeng [3].

Oztop et al. [4] using a numerical simulation studied effect of position of a heater in a cavity with cold vertical walls and adiabatic horizontal walls. Their results showed that mean Nusselt number at both vertical and horizontal location position increased with increase in Rayleigh number and length of the heater.

Tiwari and Das [5] investigated numerically the behavior of nanofluids inside a two-sided lid-driven, differentially heated, square cavity by means of the finite volume method. They developed a model to analyze the thermal behavior of nanofluids by taking into account the solid volume fraction.

Santra et al. [6] studied free convection of Cu-water nanofluid in a differentially heated square cavity with the assumption of Ostwaldede Waele non-newtonian behavior of nanofluid. They found that rate of heat transfer decreased when the nanoparticles volume fraction increased for a particular  $Ra$ .

Oztop and Abu-Nada [7], undertook a numerical study of natural convection inside a cavity, partially heated from it left side wall, by considering different nanofluids such Cu-water,  $TiO_2$ -water and  $Al_2O_3$ -water. The right wall was maintained at a constant temperature lower than that of the left discrete source, when the other walls were adiabatic. Their results show that the increase values of the nanoparticles volume fraction improve the heat transfer; the latter is most important using the Cu nanoparticles. Besides, the heat transfer rate is an increasing function of the increases source height and is more pronounced at a small aspect ratio than a large one.

Free convection fluid flow and heat transfer of various water based nanofluids in a square cavity with an inside thin heater has been investigated numerically by Mahmoodi [8]. The latter was studied a cavity with left and right walls maintained at constant temperature  $T_c$  while top and bottom walls are insulated. As result, it was observed that at low Rayleigh numbers the horizontal positioned heater have higher Nusselt number compared to the vertical positioned heater while at high Rayleigh numbers the position of the heater does not affect the heat transfer rate. Moreover, it was found

that at high Rayleigh numbers, the Ag-water nanofluid is more effective to enhance the heat transfer rate while at low Rayleigh numbers the type of nanofluids does not affect the heat transfer rate.

Mahmoodi and Sebdani [9] inspected numerically the free convection of the Cu-water nanofluid inside a differentially heated square cavity with an adiabatic square body located in its centre. For various values of the Rayleigh number, the mean Nusselt number is found increases with the increase nanoparticles volume fraction.

As such, the purpose of the present work is to investigate the natural convection phenomenon inside a square enclosure filled with CuO-water nanofluid, including two squares, a heater and a cooler mounted at center nearer the left and right side walls at a distance of 20% of the height of the cavity. The numerical results will be presented in terms of pertinent parameters such the Rayleigh number, the nanoparticles volume fraction.

## 2. Governing equations and problem formulation

### 2.1. Problem's statement

The problem under investigation, (as shown in Fig. 1), is a laminar two dimensional natural convection inside a square cavity having two isothermal squares, one heater and the other cooler (of a width  $w$  equals 20% of the cavity length), mounted at centre nearer the left and right side walls at distance of 20% of the height of the cavity respectively.

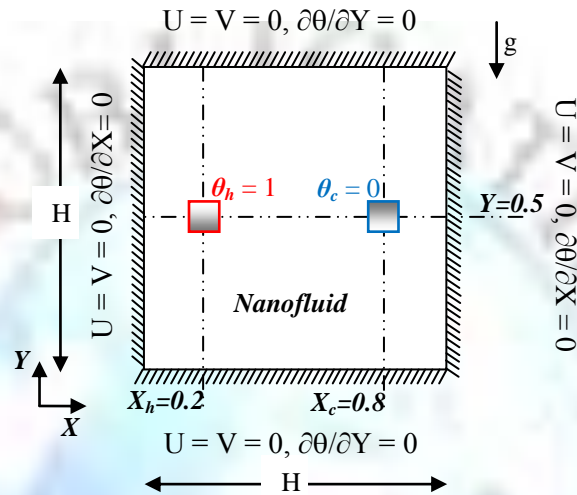


Figure 1. Simulation domain with its boundary conditions.

It is assumed that the cavity is filled with a CuO-water nanofluid, where the water and the nanoparticles are in thermal equilibrium. The computational results are obtained for a wide range of the Rayleigh number and the nanoparticles volume fraction. The constant thermo-physical properties of the base fluid and the nanoparticles are given in Table 1, whereas the nanofluid density variation in the buoyancy forces is determined using the Boussinesq approximation [10].

Table 1: Thermophysical properties of the base fluid and nanoparticles [11].

Thermo-physical properties	Fluid Phase(water)	CuO
$C_p$ (J/kg K)	4179	540
$\rho$ (kg/m <sup>3</sup> )	997.1	6510
$k$ (W/m K)	0.613	18
$\beta$ (1/K) $\times 10^{-5}$	21	0.85

### 2.2. Mathematical formulation

The nanofluid density,  $\rho_{nf}$ , heat capacity,  $(\rho C_p)_{nf}$ , thermal expansion coefficient,  $(\rho\beta)_{nf}$  and thermal diffusivity,  $\alpha_{nf}$ , are defined respectively as follows [2]:

$$\rho_{nf} = (1 - \phi)\rho_f + \phi\rho_s \quad (1)$$

$$(\rho C_p)_{nf} = (1 - \phi)(\rho C_p)_f + \phi(\rho C_p)_s \quad (2)$$

$$(\rho\beta)_{nf} = (1 - \phi)(\rho\beta)_f + \phi(\rho\beta)_s \quad (3)$$

$$\alpha_{nf} = \frac{k_{nf}}{(\rho C_p)_{nf}} \quad (4)$$

Where  $\phi$  is the nanoparticles Volume fraction and the subscripts nf, f and s designed nanofluid, fluid and solid phase respectively.

The effective viscosity of a fluid of viscosity  $\mu_f$  containing a dilute suspension of small rigid spherical particles is given by [12] as:

$$\mu_{nf} = \frac{\mu_f}{(1-\phi)^{2.5}} \quad (5)$$

The thermal conductivity,  $k_{nf}$ , of the nanofluid is obtained from the Maxwell models [13] as:

$$\frac{k_{nf}}{k_f} = \frac{(k_s + 2k_f) - 2\phi(k_f - k_s)}{(k_s + 2k_f) + \phi(k_f - k_s)} \quad (6)$$

The dimensionless conservation equations, describing the transport phenomenon inside the square, can be written as:

$$\frac{\partial U}{\partial X} + \frac{\partial V}{\partial Y} = 0 \quad (7)$$

$$U \frac{\partial U}{\partial X} + V \frac{\partial U}{\partial Y} = -\frac{\partial P}{\partial X} + \frac{\mu_{nf}}{\rho_{nf}\alpha_f} \left[ \frac{\partial^2 U}{\partial X^2} + \frac{\partial^2 U}{\partial Y^2} \right] \quad (8)$$

$$U \frac{\partial V}{\partial X} + V \frac{\partial V}{\partial Y} = -\frac{\partial P}{\partial Y} + \frac{\mu_{nf}}{\rho_{nf}\alpha_f} \left[ \frac{\partial^2 V}{\partial X^2} + \frac{\partial^2 V}{\partial Y^2} \right] + \frac{(\rho\beta)_{nf}}{\rho_{nf}\beta_f} Ra \cdot Pr \cdot \theta \quad (9)$$

$$U \frac{\partial \theta}{\partial X} + V \frac{\partial \theta}{\partial Y} = \frac{\alpha_{nf}}{\alpha_f} \left[ \frac{\partial^2 \theta}{\partial X^2} + \frac{\partial^2 \theta}{\partial Y^2} \right] \quad (10)$$

Where X, Y, U, V, P, and  $\theta$  designed, the dimensionless parameters, given by :

$$X = \frac{x}{H}; Y = \frac{y}{H}; U = \frac{uH}{\alpha_f}; V = \frac{vH}{\alpha_f}; P = \frac{pH^2}{\rho_{nf}\alpha_f^2}; \theta = \frac{T-T_c}{T_h-T_c} \quad (11)$$

The Rayleigh and Prandtl numbers are defined as:

$$Ra = \frac{g\beta\Delta TH^3}{\alpha_f\nu_f} \quad (12)$$

$$Pr = \frac{\nu_f}{\alpha_f} \quad (13)$$

The average Nusselt number for the heater  $\overline{Nu}_h$  is expressed as:

$$\overline{Nu}_h = \frac{1}{w} \int_{X_h - \frac{1}{2}}^{X_h + \frac{1}{2}} \left( \frac{k_{nf}}{k_f} \right) \left\{ \left( \frac{\partial \theta}{\partial Y} \right) \Big|_{\text{bottom}} - \left( \frac{\partial \theta}{\partial Y} \right) \Big|_{\text{upper}} \right\} dX + \frac{1}{w} \int_{Y_p - \frac{1}{2}}^{Y_p + \frac{1}{2}} \left( \frac{k_{nf}}{k_f} \right) \left\{ \left( \frac{\partial \theta}{\partial X} \right) \Big|_{\text{left}} - \left( \frac{\partial \theta}{\partial X} \right) \Big|_{\text{right}} \right\} dY \quad (14)$$

In similar way, the average Nusselt number for the cooler  $\overline{Nu}_c$  was defined similarly.

The overall mean Nusselt number is defined as:

$$\overline{Nu}_{mean} = \frac{\overline{Nu}_h + \overline{Nu}_c}{2} \quad (15)$$

### 3. Numerical procedure and validation

The governing conservation equations are discretized in space using the finite volume approach and the SIMPLER algorithm [14]. In this method, a regular two-dimensional finite difference mesh is generated in the computational domain.

In order to validate the numerical procedure, the performance of the using code via the natural convection of nanofluids is established by comparing its predictions with other numerical results, and by verifying the grid independence of the present results. This comparison it doing with the results of Arefmanesh et al. [15], for the case of a cold enclosure with a square heater was carried out by considering effects of the Rayleigh number and the TiO<sub>2</sub>-water nanofluid volume fraction on the mean Nusselt number. Fig. 2, which illustrates this comparison, shows a great agreement between both results when we taking a regular grid of 100<sup>2</sup> nodes.

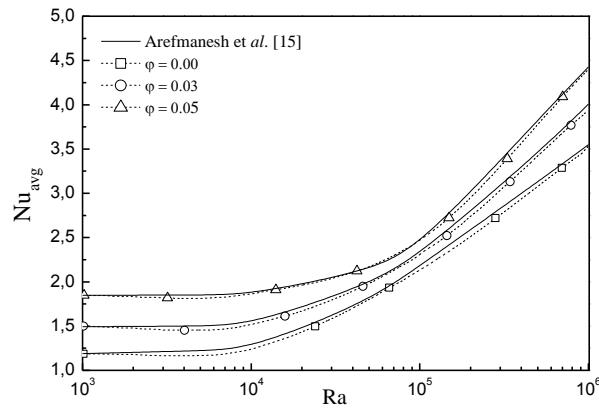


Figure 2. Average Nusselt number variation for the outer square for AR = 1/4. Comparaison with Arefmanesh et al. [15].

In order to determine a proper grid for the numerical simulation, a grid independence study is conducted for the natural convection heat transfer in the space between enclosure and the two squares (fig. 1). The grid refinement tests have been performed for five different uniform grids, namely, 41x41, 61x61, 81x81, 101x101 and 121x121 for CuO-Water nanofluid with  $\phi = 0,02$  at  $Ra=10^6$ .

The results for the average Nusselt number for the above uniform grids are presented in Table 2. It is observed that an 121x121 uniform grid is fine to capture the temperature and velocity variations in the boundary layers adjacent to the squares. Therefore, based on these results, an 121x121 uniform grid is employed to perform all of the subsequent numerical calculations.

Table 2:  $\overline{Nu}_{mean}$  for different uniform grids ( $Ra = 10^6$  and  $\phi = 0,02$ ).

Grid size	41x41	61x61	81x81	101x101	121x121
$\overline{Nu}_{mean}$	8,583	8,565	8,582	8,609	8,636

Noted that the convergence criterion for temperature, pressure, and velocity is given as:

$$\text{Error} = \frac{\sum_{j=1}^m \sum_{i=1}^n |\xi_{i,j}^{k+1} - \xi_{i,j}^k|}{\sum_{j=1}^m \sum_{i=1}^n |\xi_{i,j}^{k+1}|} \leq 10^{-6} \quad (16)$$

Where both m and n are the grid points numbers in X and Y directions, respectively.  $\xi$  is any of the computed field variables, k is the iteration number, i and j are nodes according to X and Y directions.

#### 4. Results and discussion

The presented results are generated for different pertinent dimensionless groups as: the Rayleigh number ( $10^3 \leq Ra \leq 10^6$ ) and the solid volume fraction (0% to 10%). The default parameters are assigned to the heater and colder width value  $w = 0.20$ , and the Prandtl number  $Pr = 6.2$ .

The type of nanoparticles investigated is CuO. The predicted hydrodynamic and thermal fields 'variables are presented through the streamlines, the isotherms, and the corresponding velocity profiles. The overall mean Nusselt number is also represented in order to supply useful information about the influence of each parameter, quoted above, on the mean transfer enhancement.

For each value of the Rayleigh number Ra, the streamlines and the isotherms plots of the CuO-water nanofluid with a volume fraction  $\phi = 0.10$  as well as the base fluid, ( $\phi = 0$ ) are illustrated in fig. 3.



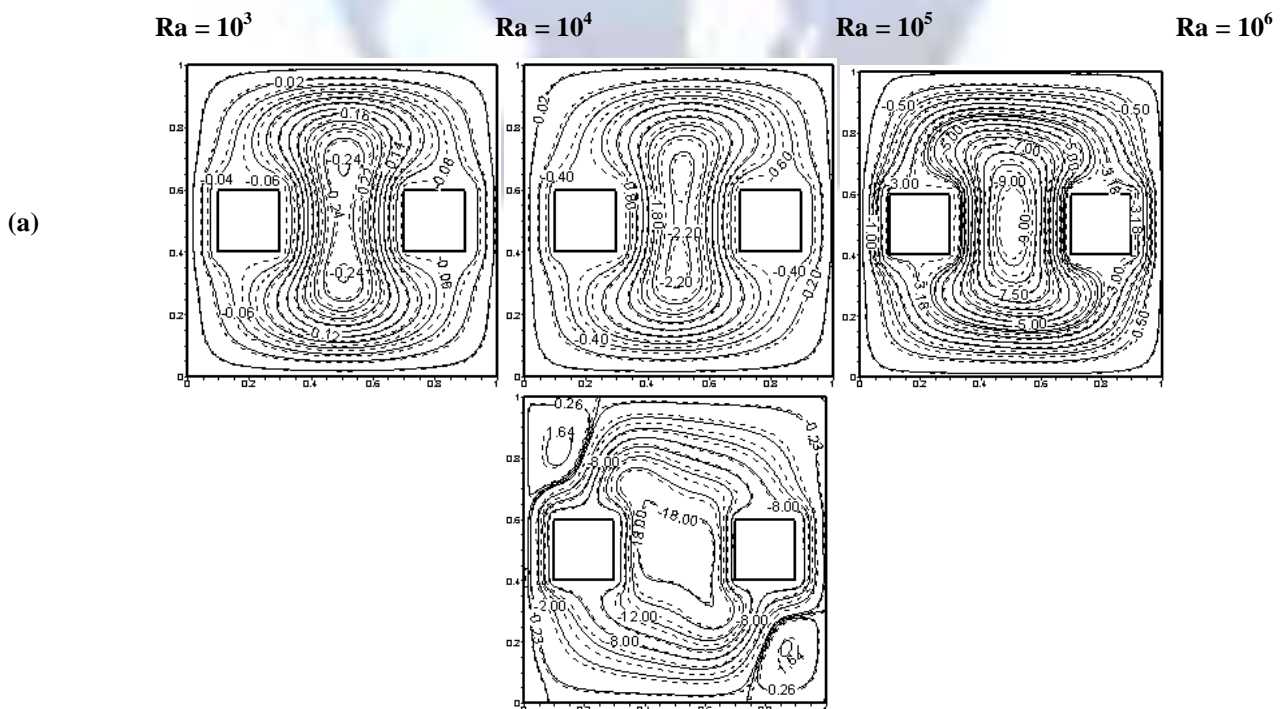
In the absence of the nanoparticles,  $\phi = 0$ , and with a low value of the Rayleigh number, which means that conduction heat transfer is dominant, the streamlines show one rotating eddy established between the heater and colder. By increasing buoyant force via increasing Rayleigh number, the flow intensity increases and two eddies are developed in at the upper left and lower right corner of the cavity. The streamlines are packed adjacent to the heater and cooler squares, transporting the hot liquid towards the upper wall near the heater and vice versa near the cooler when the liquid move downward the. As  $Ra = 10^6$ , the convection mechanism becomes more pronounced and then, the streamlines are distorted which give rise of the two eddies as depicted in fig. 3(a).

In the presence of the nanoparticles, the fluid motion is better than that of the pure fluid. In other words, the velocity components of nanofluids rise as the fluid's energy transport increases with the increase nanoparticles volume fraction. The increase in the Rayleigh number adds to the flow strength which causes, in turn, the rise in the tendency of the cell to grow.

Regarding the thermal plots in Fig. 3(b), for a Rayleigh number equals to  $10^3$ , the isotherms are uniformly distributed inside de square, revealing a dominated-conduction heat transfer regime. As the Rayleigh number increases over than  $10^4$ , the natural convection effect turns out to be dominant and then, the isotherms are distributed in a stratified manner with horizontal profile in the middle of the enclosure between the heater and cooler, whereas thin thermal boundary layers are shaped around the two squares.

Fig. 4 illustrates the vertical velocity component profiles along the horizontal plane of the cavity at  $Y_p = 0.4$  for different volume fraction and Rayleigh number of nanofluid. The examination of the magnitude of the vertical velocity component for different values of  $Ra$  confirms the weakness of the rotating eddies, clearly observed in the streamlines, for a low Rayleigh number. Besides, the vertical velocity profiles verify the existence of a clockwise circulating cell with a high magnitude between the heater and cooler compared to its magnitude close to vertical walls of cavity and the two squares. As the Rayleigh number increase, at  $Ra=10^6$  the magnitude of  $V$ -velocity between squares is nearly the same in the corner close to vertical walls owing to the thermal buoyancy effects.

Fig. 5 displays the mean Nusselt number calculated along the two squares sides with respect to the solid volume fraction at various values of the Rayleigh number. In general, the mean Nusselt number is an increasing function of the Rayleigh number as the convective regime becomes dominates and increases with the increase of the nanoparticles volume fraction, due to the improvement of the fluid thermal conductivity. For  $\phi = 0.10$ , the mean Nusselt number is doubled when the Rayleigh number increase from  $10^5$  to  $10^6$ .



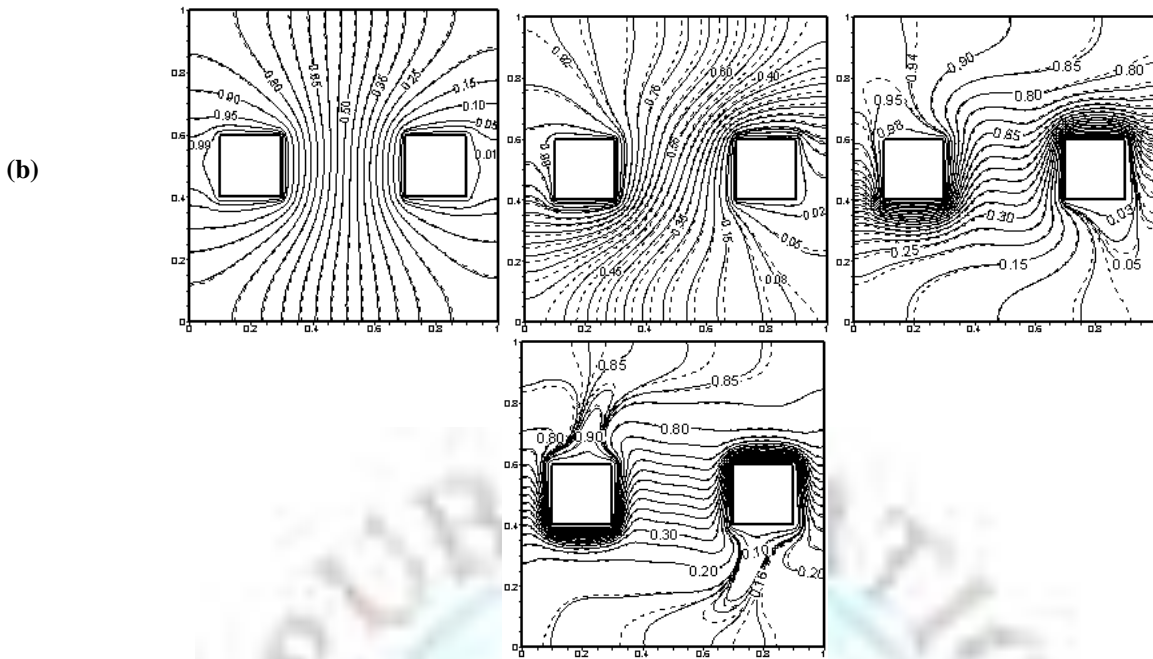


Figure 3. Streamlines (a) and isotherms (b) plots for different values of the Rayleigh number [ ---  $\phi = 0.10$ , — base fluid].

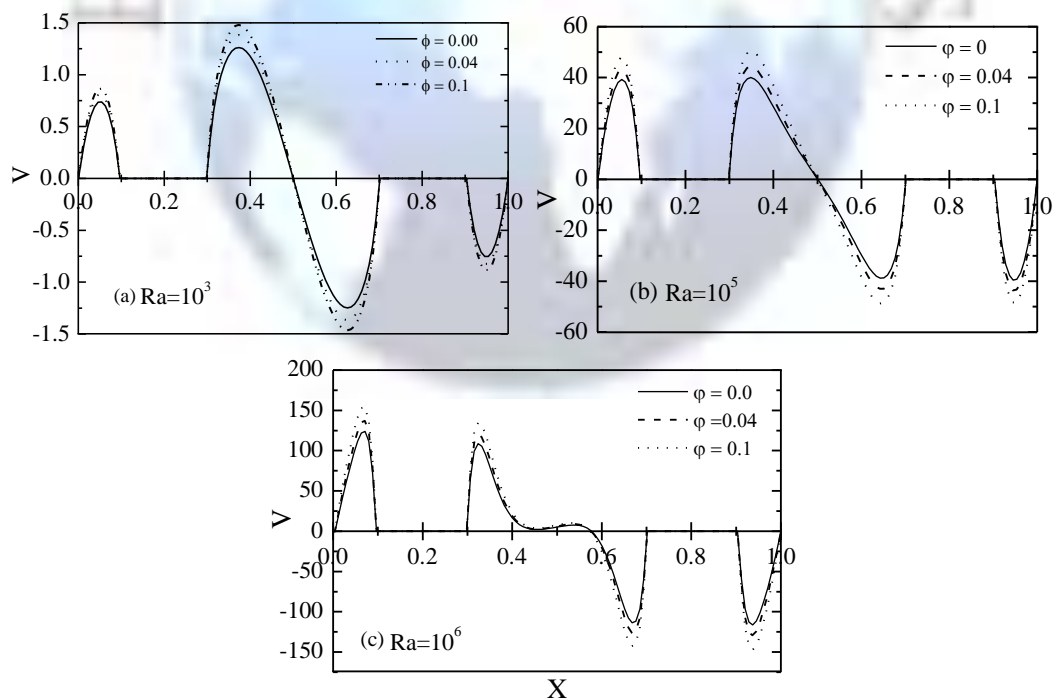


Figure 4. Vertical velocity profiles at position  $Y_p = 0.4$  for different values of the Rayleigh number and volume fraction of nanoparticle.

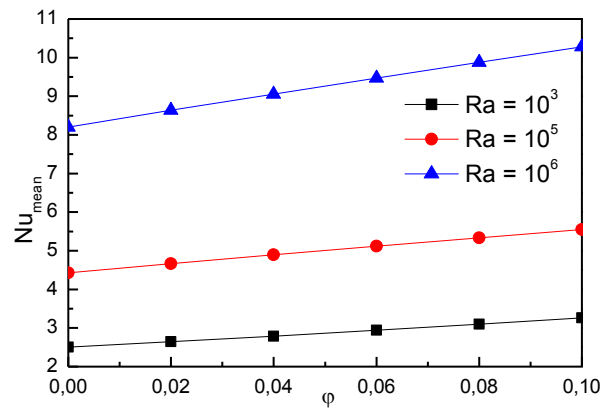


Figure 5. Variation of the mean Nusselt number with the nanoparticles volume fraction for various values of the Rayleigh number.

## 5. Conclusions

The analysis of nanofluids natural convection inside a square enclosure, including two squares heater and cooler, was numerically studied in this paper. Focusing specially on the effects of Rayleigh number and volume fraction of nanoparticles CuO.

The results may resume as follows:

- For the investigated nanofluid, heat transfer is found as an increasing function of the Rayleigh number and the nanoparticles volume fraction.
- For a higher Rayleigh number, the natural convection effect turns out to be dominant and then, the isotherms are distributed in a stratified manner between the heater and cooler, whereas thin thermal boundary layers are shaped around the two squares.
- The mean Nusselt number is an increasing function of the Rayleigh number as the convective regime becomes dominates and increases with the increase of the nanoparticles volume fraction, due to the improvement of the fluid thermal conductivity.

## References

- [1]. S. Ostrach "Natural convection in enclosures", Journal of Heat Transfer 110 (4) 1175-1190 (1988).
- [2]. K. Khanafer, K. Vafai, M. Lightstone "Buoyancy-driven heat transfer enhancement in a two-dimensional enclosure utilizing nanofluids", International Journal of Heat and Mass Transfer (46) 3639-3653 (2003).
- [3]. Jou, R.Y., Tzeng, S.C. "Numerical research of nature convective heat transfer enhancement filled with nanofluids in rectangular enclosures" International Communications in Heat and Mass Transfer, Vol. 33, pp. 727-736 (2006).
- [4]. H.F. Oztop, I. Dagtekin, A. Bahloul "Comparison of position of a heated thin plate located in a cavity for natural convection" Int. Commun. Heat Mass Transfer 31 (2004) 121-132 (2004).
- [5]. Tiwari, R.K., Das, M.K. "Heat transfer augmentation in a two-sided lid-driven differentially heated square cavity utilizing nanofluids" International Journal of Heat and Mass Transfer, Vol. 50, pp. 2002-2018 (2007).
- [6]. A.K. Santra, S. Sen, N. Chakraborty "Study of heat transfer in a differentially heated square cavity using copper-water nanofluid" International Journal of Thermal Science (48) 1113-1122 (2008).
- [7]. H.F. Oztop, E. Abu-Nada "Numerical study of natural convection in partially heated rectangular enclosures filled with nanofluids", Int. J. Heat Fluid Flow (29) 1326-1336 (2008).
- [8]. M. Mahmoodi "Numerical simulation of free convection of nanofluid in a square cavity with an inside heater" International Journal of Thermal Sciences (50) 2161-2175 (2011).
- [9]. M. Mahmoodi, S.M. Sebdani "Natural Convection in a Square Cavity Containing a Nanofluid and an Adiabatic Square Block at the Centre", Superlattices and Microstructures, 52(2):261-275 (2012).
- [10]. Bejan, A. "Convection heat transfer", John Wiley & Sons, Inc., Hoboken, New jersey, USA, 2004.
- [11]. Abu-Nada E., Masoud Z., Oztop H.F., Campo A. "Effect of nanofluid variable properties on natural convection in enclosures", International Journal of Thermal Sciences (49) 479-491 (2010).
- [12]. Brinkman, H.C. "The viscosity of concentrated suspensions and solutions", Journal of Chemical Physics, Vol. 20, pp. 571-581 (1952).
- [13]. Maxwell, J.C. "A Treatise on Electricity and Magnetism", vol. II, Oxford University Press, Cambridge, U.K, pp. 54 (1873).
- [14]. S.V. Patankar "Numerical Heat Transfer and Fluid Flow", Hemisphere Publishing Corporation, Taylor and Francis Group, New York, 1980.
- [15]. Arefmanesh, A., Amini, M., Mahmoodi, M., Najafi, M. "Buoyancy-driven heat transfer analysis in two-square duct annuli filled with a nanofluid", European Journal of Mechanics B-Fluids, 33, pp. 95-104 (2012).